



The synergistic roles of MsRCI2B and MsRCI2E in the regulation of ion balance and ROS homeostasis in alfalfa under salt stress

Depeng Zhang^a, Zhongbao Shen^b, Pin He^a, Jianli Wang^b, Donghuan Li^a, Jing Meng^a, Dongmei Zhang^b, Jia You^b, Yaqin Luo^a, Xinsheng Wang^a, Xu Zhuang^b, Linlin Mu^b, Shichao Zhang^a, Weibo Han^{b,*}, Hua Cai^{a,*}

^a College of Life Science, Northeast Agricultural University, Harbin 150030, China

^b Institute of Forage and Grassland Science, Heilongjiang Academy of Agricultural Sciences, Harbin 150086, China



ARTICLE INFO

Keywords:

Medicago sativa

RCI2

Salt stress

ABSTRACT

Under salt stress, plasma membrane proteins regulate ion homeostasis and the balance between reactive oxygen species (ROS). In this study, we investigated the functions of two small membrane proteins—MsRCI2B (tailless) and MsRCI2E (tailed)—encoded by the *RCI2* (Rare Cold Inducible 2) gene family in *Medicago sativa* (alfalfa). We identified the distinct subcellular localization and expression patterns of these proteins under salt stress. Using yeast two-hybrid (Y2H), GST pull-down, and bimolecular fluorescence complementation (BiFC) assays, we confirmed the physical interactions between MsRCI2B and MsRCI2E. Transgenic alfalfa lines overexpressing *MsRCI2(OE#RCI2)* and co-expressing both *MsRCI2B* and *MsRCI2E* (*OE#RCI2E-2B*) were developed to explore their roles in salt tolerance. Interestingly, the C-terminal tail of MsRCI2E negatively affects salt tolerance; however, its interaction with MsRCI2B mitigates this adverse effect. To further understand the regulatory mechanisms, we screened for plasma membrane proteins (PMPs) that interact with MsRCI2B or MsRCI2E using a DUALmembrane yeast two-hybrid system. MsCaM1 interacts with MsRCI2B, whereas MsPIP1;4 and MsHVP1 specifically interact with MsRCI2E. Notably, the MsRCI2E-PIP1;4 interaction influenced the intracellular trafficking of PIP1;4, reducing its presence on the plasma membrane and thereby limiting the export of H₂O₂, which helps maintain ROS homeostasis. Additionally, the interaction between MsRCI2E and HVP1 stabilized ion homeostasis by decreasing Na⁺ concentration in the cytoplasm under salt stress. Overall, our study provides new insights into the molecular mechanisms through which MsRCI2B and MsRCI2E coordinate the ion and ROS balance under salt stress and offering promising strategies for enhancing crop tolerance to salinity.

1. Introduction

Alfalfa (*Medicago sativa* L.) is a perennial leguminous plant recognised for its high nutritional value, substantial yield, broad geographical distribution, and adaptability to diverse environmental conditions. Despite its moderate salinity tolerance, alfalfa yield declines significantly in high-salinity regions [1]. Therefore, enhancing alfalfa yields in mildly saline soils is crucial for soil reclamation and the advancement of animal husbandry.

High salt concentrations induce ionic toxicity and osmotic stress [2,3]. Excess sodium ions (Na⁺) stimulate the accumulation of reactive oxygen species (ROS), leading to oxidative stress in plants. Plants have developed defence mechanisms to regulate ion balance and manage

ionic and oxidative stress. Plasma membrane proteins are crucial in sensing and transmitting high-salt signals, such as the calcium-binding protein SOS3, Na⁺/H⁺ transporter SOS1, and HKT1 in the SOS pathway [4,5]. In addition, studies have shown that plasma membrane proteins PIP2 [6], H⁺-ATPase [7,8], and calmodulin (CaM) [9] play important roles in the salt stress response.

RCI2 (Rare Cold-Inducible Protein 2) is a plasma membrane protein that is significantly induced by salt, low temperature, and drought. Arabidopsis plants overexpressing *AtRCI2* exhibit enhanced resistance to high salinity, demonstrating less growth inhibition and reduced Na⁺ accumulation [10]. Furthermore, increased exogenous Na⁺ levels resulted in reduced potassium (K⁺) content in the roots and shoots of *rci2a* mutants [11]. These findings suggested that *RCI2* plays a crucial role in the

* Corresponding authors.

E-mail addresses: hanweibo@haas.cn (W. Han), caihua@neau.edu.cn (H. Cai).

regulation of cation homeostasis. In addition to maintaining plasma membrane stability, RCI2 may influence membrane fluidity under salt stress. Studies have indicated that membrane fluidity in wild-type *Arabidopsis* under high Na⁺ or K⁺ conditions is significantly greater than in *rci2a* mutants, but lower than that in transgenic plants expressing 35S: *MpRCI* [12]. Moreover, RCI2 has been proposed to stabilise the plasma membrane and prevent damage during cold stress [13,14].

Overall, the significance of the RCI2 protein in mitigating salt, drought, and cold stress is evidenced by *RCI2* gene overexpression in transgenic plants [15–17]. Recent discoveries of RCI2 class genes across various plant species have revealed their functional specificity [18–20]. Understanding the specific functions of RCI2 proteins requires an examination of their unique structural features. RCI2 proteins possess two transmembrane domains (TMD) and a hydrophilic C-terminal region. *Arabidopsis RCI2* genes can be classified into two groups based on the presence of a hydrophilic C-terminus following the second TMD: tail-type (*AtRCI2D/E/F/G*) and tailless-type (*AtRCI2A/B/C/H*) [21]. The role of C-terminal in complementation of NaCl sensitivity in *pmp3* yeast mutants is well-documented, tailless RCI2 proteins can complement $\Delta pmp3$ yeast tolerance to NaCl, while tailed RCI2 proteins failed to do so [19]. *AtRCI2D* (75 aa, tail-type) does not complement $\Delta pmp3$ yeast, whereas its deletion isoform *AtRCI2D-D1* (57 aa, tailless-type) succeeds [21]. Despite these insights, the functional differences between tailed and tailless RCI2 proteins under stress conditions in plants remain unclear.

Long et al. [22] identified five *RCI2* genes from *Medicago truncatula* and cloned *MsRCI2A* from *Medicago sativa*. Their *pmp3* yeast complementation and green fluorescence protein (GFP) fusion experiments revealed that *MtRCI2A-2C* can complement yeast *pmp3* mutants and localise in the cell membrane, whereas *MtRCI2D* and *MtRCI2E* fail to complement $\Delta pmp3$ and are localised in both the cell membrane and intracellular membranes, including the endoplasmic reticulum (ER) [23]. Previous studies that transformed five *MsRCI2* genes into alfalfa showed differential salt and alkali tolerance among transgenic plants. Additionally, differences in the transcriptional regulation of ion channel-related genes (*H⁺-ATPase*, *SOS1*, *NHX1*, etc.) by *MsRCI2* were observed. However, the molecular mechanisms underlying the functional specificity of tailed and tailless *RCI2* genes remain unclear [24,25]. Thus, this study aims to systematically compare the functional differences between *MsRCI2B* (54 aa, tailless) and *MsRCI2E* (76 aa, tailed) in response to salt stress. We will investigate their roles in salt tolerance in transgenic alfalfa through analyses of gene expression, protein localization, and protein interactions. The objectives of this study were to elucidate the molecular mechanisms governing salt stress tolerance in alfalfa and identify candidate genes for improving alfalfa cultivars.

2. Materials and methods

2.1. Plant materials and growth conditions

Germinated seeds of Alfalfa (*Medicago sativa* "Longmu 806") were cultivated in plastic pots filled with a 1:1 (v/v) mixture of vermiculite and perlite. The greenhouse conditions were maintained at 24 ± 2 °C with a 16-h light and 8-h dark cycle and a relative humidity of 55 %. During the initial growth phase, both the control and abiotic stress treatment groups received a 1/5 strength Hoagland nutrient solution. After approximately one month of cultivation, alfalfa lines exhibiting similar growth status were selected for further experimentation.

The seedlings were subjected to treatments with salt (200 mmol/L NaCl), alkali (200 mmol/L NaHCO₃, pH 8.5), salicylic acid (SA, 100 µmol/L), and hydrogen peroxide (H₂O₂, 100 µmol/L) for durations of 0, 1, 3, and 6 h, after which leaf samples were collected.

Given the low natural pollination rate of alfalfa, seed propagation under laboratory conditions poses challenges. Therefore, this study employed asexual propagation techniques to reproduce both wild-type (WT) and transgenic lines (OE#*RCI2*). The plants were irrigated with a 200 mmol/L NaCl solution at a dose of 200 mL per pot once for salt treatment.

2.2. Gene cloning and sequence identification

Full-length amplification primers for *MsRCI2B* and *MsRCI2E* were designed based on the nucleic acid sequences of *MtRCI2B* (Medtr7g111350) and *MtRCI2E* (Medtr4g130660). These primers are detailed in Supplementary Table S1. Phylogenetic analysis of *MsRCI2A/B/C/D/E/F*, yeast *PMP3* (DB661484), wheat *WPI6* (AB030210), rice *OsLti6a/b* (AY607689, AY607690), *Arabidopsis AtRCI2A/B/C/D/E/F/G/H* (AT3G05880, AT3G05890, AT1G57550, AT2G24040, AT4G30650, AT4G30660, AT4G28088, AT2G38905), and *Camelina sativa RCI2A/E* (JQ809231, JQ809232) was performed using MEGA software. Multiple sequence comparisons of *RCI2* genes were conducted using DNAMAN version 8.0 (Lynnon Biosoft) with default parameters. Phylogenetic trees were constructed using MEGA 6.2 (<http://www.mega-software.net/>) applying the Neighbor-Joining method. All DNA sequences were translated into amino acid sequences for analysis.

2.3. RNA extraction, cDNA synthesis, and quantitative real-time PCR (RT-qPCR)

Total RNA was extracted from the leaves, stems, and roots of 1-month-old wild-type and transgenic alfalfa lines. Plants were treated with salt, alkali, SA, and H₂O₂ solutions, and roots or leaves were collected. The Plant RNAPrep Pure Kit (Kangwei, China) was used to extract total RNA according to the protocol. The extracted RNA was analyzed using a 2.0 % agarose gel and quantified with a NanoDrop ND-1000 spectrophotometer (NanoDrop, Wilmington, USA). The first strand cDNA was immediately synthesized using the reverse transcription kit (Vazyme, China). Gene-specific primers, designed using PrimerBLAST (<https://www.ncbi.nlm.nih.gov/tools/primer-blast/>), are listed in Supplementary Table S1. RT-qPCR was performed in a 96-well (10 µL) format using Trans Start Top Green qPCR SuperMix (Vazyme Biotech, Nanjing, China), with *GAPDH* as the internal reference gene. The relative expression level was calculated using the 2^{-ΔΔCT} method with three biological replicates per sample to ensure statistical significance.

2.4. Subcellular localization

For double enzyme cleavage of p2300 mCherry, the *Bam* H I and *Kpn* I cleavage sites were selected. Following the one-step cloning kit protocol from Vazyme was ligated to a linear vector and transferred to *E. coli* DH5α. Correct clones were identified, and the resulting constructs were introduced into *Agrobacterium tumefaciens* strain GV3101. Agrobacterial cells were suspended in infiltration buffer containing 10 mmol/L MgCl₂, 10 mmol/L MES, and 150 µmol/L acetosyringone (pH 5.7). After infiltration into 4-week-old *Nicotiana benthamiana* leaves, mCherry fluorescence signals were observed and measured after 48 h using a confocal laser scanning microscope. The intensity correlation analysis function of ImageJ will determine the membrane-to-cytoplasm ratio, ensuring consistent fluorescence acquisition parameters, as detailed in Schneider et al. [26].

2.5. Protein interaction

Yeast two-hybrid (Y2H) assays were conducted to examine the interaction between *MsRCI2* and other membrane protein in yeast cells using DUALmembrane system. The *Sfi* I site was selected as the single-enzyme cleavage site of pBT3-N vector, while the *Sma* I site was used for the pPR3-N vector. *MsRCI2* and the membrane proteins were ligated with a linear vector according to the one-step cloning kit from Vazyme (Beijing, China), and transfected into DH5α. The resulting constructs were introduced into the yeast strain Y2HGold via co-transformation. The transformants were cultured on a selective synthetic dropout (SD) medium lacking leucine (Leu) and tryptophan (Trp) (SD/-Leu/-Trp). The yeast colonies were re-streaked onto dropout medium (SD/-Leu/-Trp/-His) containing 3 mmol/L 3-AT and grown for 5–7 days at room

temperature.

Bimolecular fluorescence complementation (BiFC) assay was performed to observe the physical interaction between MsRCI2 and membrane proteins in viable plant cells. The coding sequences of MsRCI2 and membrane proteins were individually inserted into the C-terminal of NYFP and cYFP. The single construct vector were introduced into *Agrobacterium tumefaciens* strain GV3101. Two positive clones of GV3101 were mixed in equal amounts, and the agrobacterial cells were suspended in an infiltration buffer. The suspensions were infiltrated into 4-week-old *Nicotiana benthamiana* leaves. After 48 h, YFP fluorescence signals in the tobacco leaves were observed and measured under a confocal laser scanning microscope.

GST-pull down assay was conducted to observe the interaction between MsRCI2E and MsRCI2B in vitro. The vector pET1932 and pGEX-4 T were digested by *Eco R V* and *Sma I*, respectively. The coding sequences of MsRCI2B/E was ligated to a linear vector by one-step cloning. The recombinant GST-MsRCI2E and His-MsRCI2B was induced to express by Isopropylthiogalactoside (IPTG) in BL21 (DE3) *E. coli*. The cells were sonicated and centrifuged to remove impurities, and the supernatants were collected as total proteins. The MsRCI2B/2E protein fused with His tag or GST was purified using tag affinity purification methods with Ni-NTA agarose beads or glutathione-Sepharose 4B beads, respectively. Equal amounts of GST-MsRCI2E and His-MsRCI2B proteins were incubated with the respective beads in binding buffer (20 mmol/L Tris-HCl [pH 7.5], 150 mmol/L NaCl, 1 mmol/L EDTA, 1 % Triton X-100, and

5 % glycerol) at 4 °C for 2 h. The beads were then pelleted and washed for five times with binding buffer before being boiled in 1 × SDS loading buffer for 5 min. The proteins were fractionated using SDS-PAGE gel and transferred onto a polyvinylidene difluoride (PVDF) membrane. The membrane was immunoblotted with antibodies specific to the anti-His or GST epitopes.

2.6. Generation of transgenic alfalfa

The coding sequence of MsRCI2s-GFP/mCherry or another gene driven by the CaMV 35S promoter was cloned into the pMDC123 binary expression vector (35S::Gene-GFP/Cherry). To construct a dual-gene co-expression vector, one gene fragment from 35S::Gene-GFP/Cherry was amplified and ligated into another gene expression vector using one-step cloning approach. The resulting constructs were introduced into the *Agrobacterium rhizogenes* LBA4404 strain for transformation into the Longmu 806 cultivar using the cotyledonary node transformation system. Selection of resistant plants was carried out using 1.0 mg/L glufosinate-ammonium [24,25].

Semi-quantitative RT-PCR and quantitative real-time RT-PCR were performed to detect the mRNA expression levels of *MsRCI2* in transgenic alfalfa. Gene-specific primers were designed using Primer 5.0 software (Table S1), and the reaction specificity was assessed by examining the melting curves of RT-PCR products. The relative expression level was calculated using the $2^{-\Delta\Delta Ct}$ method, with three biological replicates

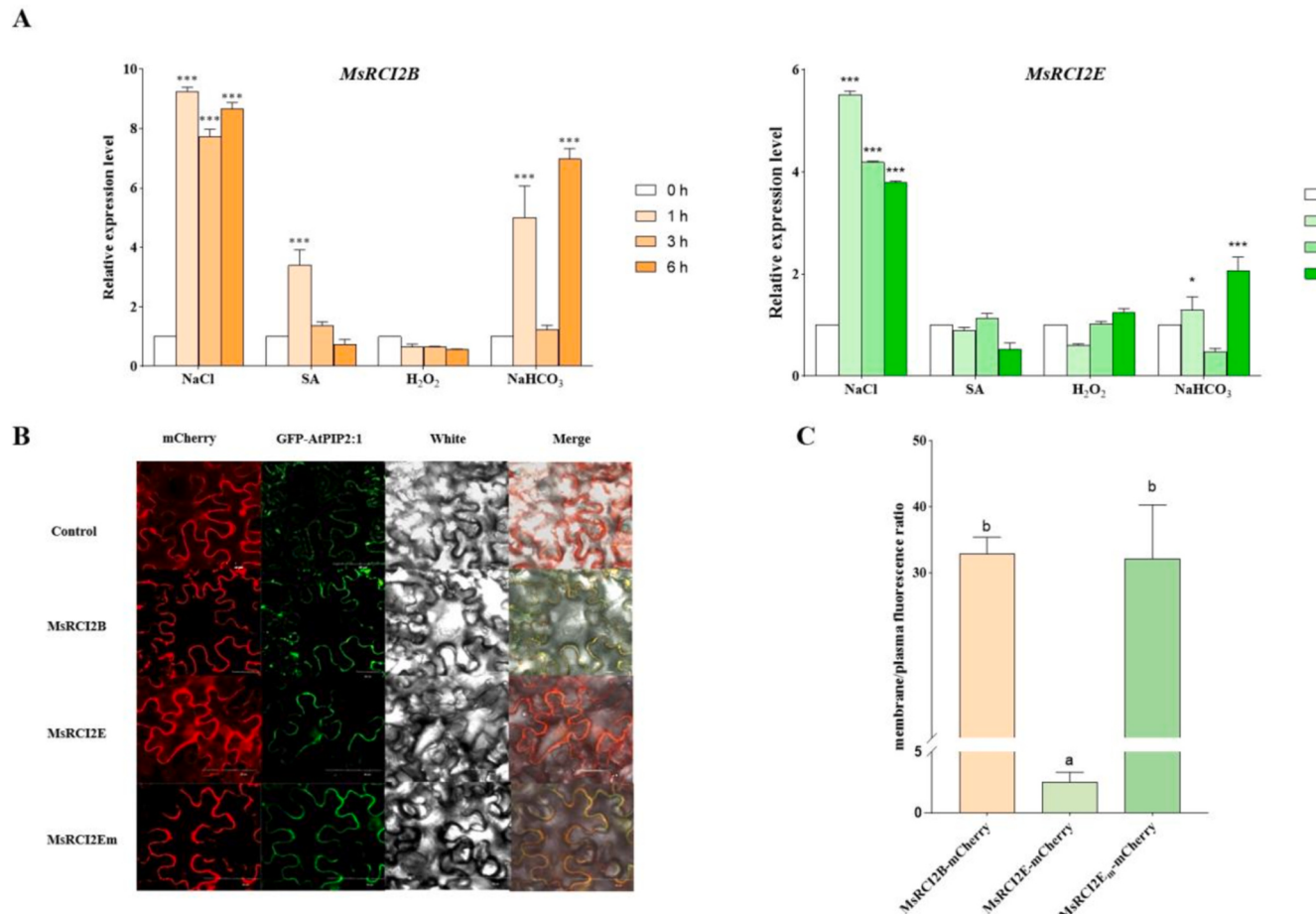


Fig. 1. Expression patterns and subcellular localization of MsRCI2B/E.

(A) Expression levels of *MsRCI2B* and *MsRCI2E* in response to salt, salicylic acid, H₂O₂, and alkali treatments, as determined by RT-qPCR analysis.

(B) Subcellular localization of the MsRCI2B/E/Em-mCherry fusion protein.

(C) Membrane/plasma fluorescence ratio of the MsRCI2B/E/Em-mCherry fusion protein.

Each experiment was performed in triplicate, yielding consistent results. Different letter indicates significant differences according to Duncan's multiple range test at $p < 0.05$ using One-way ANOVA.

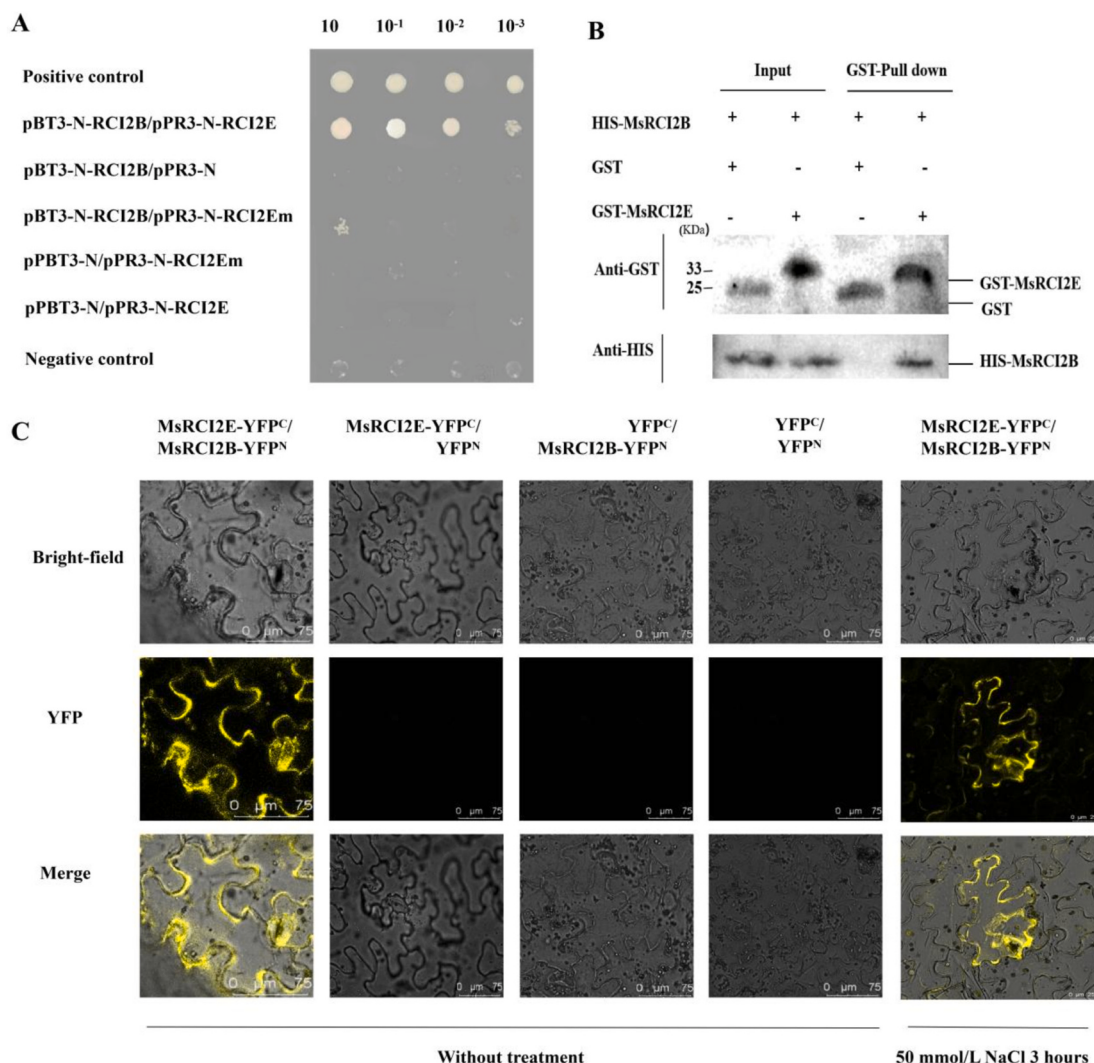


Fig. 2. Interaction between MsRCI2B and MsRCI2E.

(A) Yeast two-hybrid assay demonstrating the interaction of MsRCI2B with MsRCI2E. NMY52 cells co-transformed with pBT3-N and pPR3-N plasmids were cultured on SD/-Leu/-Trp or SD/-Leu/-Trp/-His/-Ade media.

(B) GST pull-down assay confirming the interaction between MsRCI2B and MsRCI2E. Purified His-MsRCI2B was incubated with GST or GST-MsRCI2E bound to glutathione Sepharose 4B beads. Interaction was detected by Western blotting using anti-HIS and anti-GST antibodies.

(C) BiFC assay illustrating the interaction of MsRCI2B with MsRCI2E. *MsRCI2B* and *MsRCI2E* were cloned into vectors containing YFPN or YFPC sequences. The resulting plasmids were co-expressed in tobacco leaves for 16 h, and YFP signals were observed using a confocal microscope.

employed for each sample to ensure statistical significance.

2.7. Evaluation of salt tolerance

Wild-type (WT) and transgenic plants were subjected to a 200 mmol L⁻¹NaCl solution. The relative chlorophyll content in the leaves was measured using a chlorophyll analyzer (TYS-B) at 11 a.m. on the sixth day of salt stress, under full sunlight. Relative conductivity, proline (Pro), soluble sugar, and malondialdehyde (MDA) contents were measured to complement the phenotypic analysis and evaluate the salt tolerance of the transgenic plants. Relative conductivity was determined using the vacuum infiltration method. MDA, Pro, and soluble sugar contents were analyzed using physiological kit (Suzhou Keming Biotechnology Co., Ltd., China), with measurements conducted on a UV-visible spectrophotometer. Antioxidant enzymes activities were also evaluated following salt treatment. The activities of superoxide dismutase (SOD), peroxidase (POD), and catalase (CAT) were measured using the physiological kits, while hydrogen peroxide (H₂O₂) and oxygen free radical (OFR) contents were detected and quantified using a UV-visible spectrophotometer. Plant materials were then subjected to in

diaminobenzidine (DAB), nitroblue tetrazolium (NBT) staining solution, placed in a vacuum for 30 min, and stained overnight. The next day, stained leaves were transferred to a decolorizing solution (ethanol: acetic acid: glycerol = 3:1:1) and boiled in water bath until all chlorophyll residues were removed.

2.8. Determination of Na⁺ and K⁺ content

To prepare the standard solution, 1.907 g of analytical grade KCl and 0.6355 g of NaCl were weighed and dissolved in deionized water to a final volume of 1 L. Leaves and roots of WT and transgenic alfalfa were initially dried at 105 °C, followed by further drying in an oven at 80 °C until a constant weight was achieved. A 0.05 g sample was weighed from each dried plant material. The nitration solution was prepared by mixing 5 mL of concentrated nitric acid, 1 mL of 60 % trichloroacetic acid, and 0.5 mL of concentrated sulfuric acid. This solution was added to the sample, which was subsequently extracted in a constant-temperature water bath at 90 °C. The resulting solution was filtered and analyzed for Na⁺ and K⁺ content using flame atomic absorption spectrometry.

2.9. Statistical analysis

All experiments in this study were performed in triplicate, and the average of the three measurements was calculated for analysis. GraphPad Prism 9.0 was used for graphical analysis, while one-way ANOVA was employed for significance testing ($p < 0.001$ represented by ***, $p < 0.01$ represented by ** $p < 0.05$ represented by *).

3. Results

3.1. Cloning and identification of *MsRCI2B* and *MsRCI2E* gene

MsRCI2B and *MsRCI2E* were amplified using cDNA as a template, resulting in 165 bp and 231 bp fragments, respectively. Compared to other members of the RCI2 gene family, including *MtRCI2s* and *AtRCI2*, both *MsRCI2B* and *MsRCI2E* retain the characteristic features of PMP3 proteins, such as two putative transmembrane domains (TMD), as indicated by arrows in Fig. S1A. The amino acid sequence similarity between *MsRCI2B* and *MsRCI2E* was 55.76 %, with *MsRCI2E* containing

an additional 20 hydrophilic amino acid C-terminal tails following the second TMD, therefore, *MsRCI2E* was classified as tailed-RCI2. Phylogenetic analysis (Fig. S1B) categorized these proteins into two distinct groups based on their branching patterns. *MsRCI2A-C* from alfalfa and *AtRCI2A-B* from *Arabidopsis* were grouped into one branch, while *MsRCI2D-F* and *AtRCI2C-H* formed another branch.

3.2. Differential expression and subcellular localization of *MsRCI2B* and *MsRCI2E*

To explore the differences in abiotic stress responses between tailless *MsRCI2B* and tailed *MsRCI2E*, we analyzed their gene expression under treatments with 100 $\mu\text{mol/L}$ SA, 200 mmol/L NaCl, 200 mmol/L NaHCO_3 , and 100 $\mu\text{mol/L}$ H_2O_2 (Fig. 1A). After NaCl treatment, the expression of *MsRCI2B/E* peaked after 1 h of treatment. For the NaHCO_3 treatment, both *MsRCI2B/E* initially decreased but subsequently increased, reaching peak levels at 12 h. In contrast, exogenous SA treatment resulted in distinct expression patterns, with *MsRCI2B* showing significant upregulation, peaking at 1 h and then decreasing.

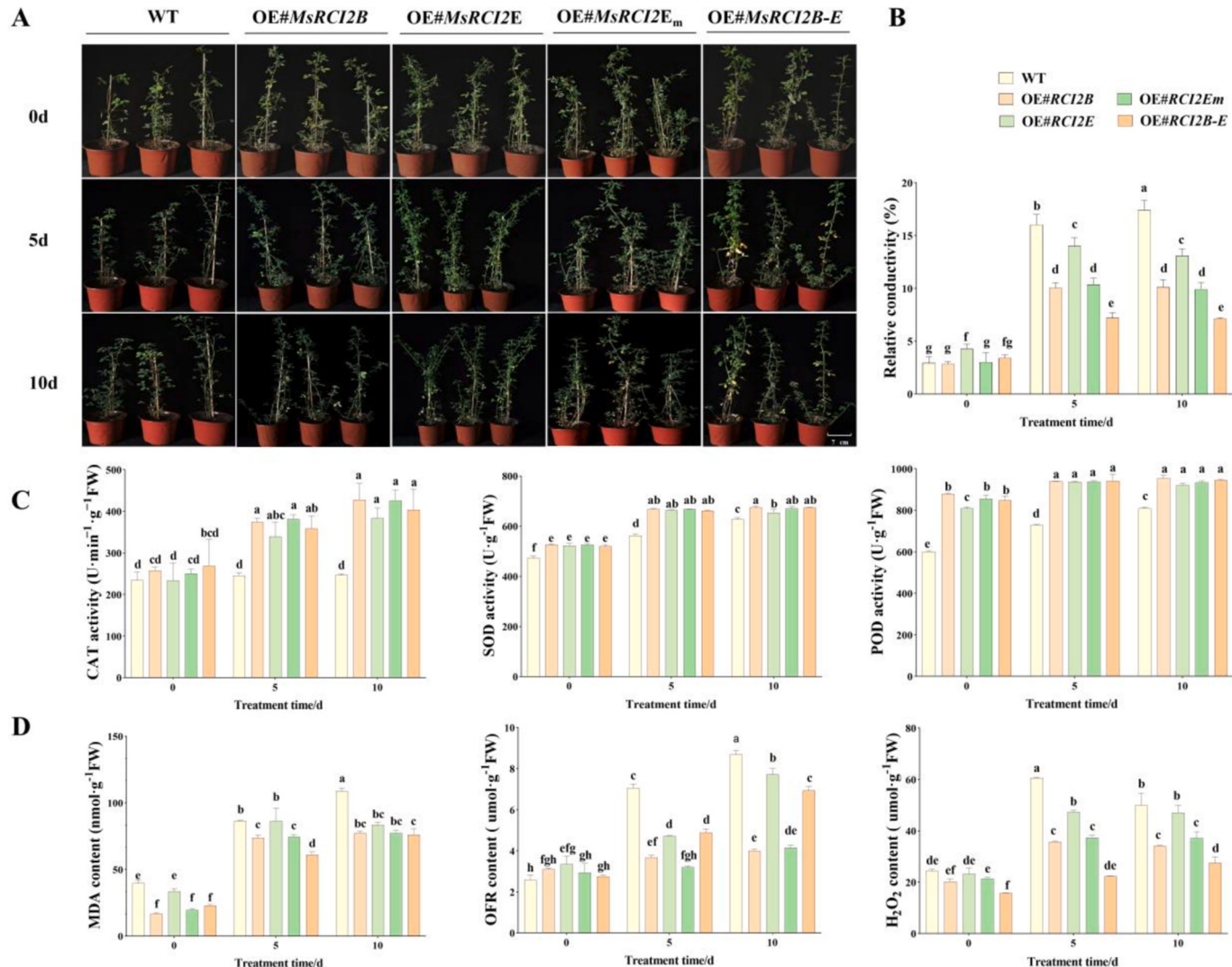


Fig. 3. Overexpression of *MsRCI2B*, *MsRCI2E* and *MsRCI2E/B* improved salt tolerance in alfalfa.

(A) Growth morphology of wild-type (WT) and transgenic lines (OE#RCI2) under salt stress.

(B) Relative conductivity of WT and OE#RCI2 lines.

(C) Catalase (CAT), superoxide dismutase (SOD), and peroxidase (POD) enzyme activity.

(D) Malondialdehyde (MDA), oxygen free radical (OFR), and H_2O_2 content. Each experiment was conducted in triplicate, with at least three technical replicates. Different letter indicates significant differences according to Duncan's multiple range test at $p < 0.05$ using One-way AMOVA.

The expression levels of *MsRCI2B/E* did not change significantly after H₂O₂ treatment.

We investigated the subcellular localization of tailless MsRCI2B and tailed MsRCI2E using 35S:mCherry fusion fluorescent proteins, including MsRCI2Em (a C-terminal tail-deleted variant of MsRCI2E). As shown in Fig. 1B, the MsRCI2B-mCherry fusion protein was exclusively localised to the plasma membrane (PM), whereas the MsRCI2E-mCherry fusion protein was observed in both the PM and intracellular compartments. The MsRCI2Em-mCherry fusion protein was predominantly localised in the PM. Analysis using ImageJ software (Fig. 1C) revealed that the membrane-to-cytoplasm ratios of MsRCI2B and MsRCI2Em were significantly higher than that of MsRCI2E ($p < 0.001$). These results indicate that tailless RCI2 proteins were primarily localised to the plasma membrane. In contrast, tailed RCI2 proteins were found in the internal membranes. This observation aligns with previous localization studies of CsRCI2F [27].

3.3. Protein interaction between MsRCI2B and MsRCI2E

We cloned six RCI2 genes (*MsRCI2A-F*) from alfalfa and validated their interactions using a DUAL membrane yeast two-hybrid (Y2H) system (Fig. S2). Only yeast cells harbouring the RCI2A/B/D-pBT3-N and RCI2E-pPR3-N pairs grew on SD/-Leu-Trp-His containing 3 mM 3-AT for high stringency, even at a 1000-fold dilution. This suggests that MsRCI2E interacts heterologously with MsRCI2A/B and MsRCI2D to form heterodimers but does not form homodimers. We further explored the RCI2B-RCI2Em interaction; however, yeast cells harbouring RCI2B-pBT3-N and RCI2Em-pPR3-N did not grow on SD/-Leu-Trp-His medium (Fig. 2A), indicating that deletion of the C-terminal tail of MsRCI2E prevented its interaction with MsRCI2B. To further validate this interaction, we expressed and purified GST, GST-MsRCI2E, and His-MsRCI2B recombinant proteins from the *E. coli* system for in vitro GST pull-down assays. Biochemical data showed that GST-MsRCI2E, but not GST, specifically pulled His-MsRCI2B down (Fig. 2B). This indicated that MsRCI2B physically interacts with MsRCI2E in vitro.

MsRCI2B is localised in the plasma membrane (PM), whereas MsRCI2E is localised within the cell. Bimolecular fluorescence complementation (BiFC) was used to study their interactions and localization. When the MsRCI2E-YFP^C and MsRCI2B-YFP^N fusion proteins were transiently co-expressed in tobacco leaf cells, yellow fluorescence was observed in the plasma membrane (Fig. 2C), indicating that the interaction between MsRCI2B and MsRCI2E was concentrated in the PM. Moreover, after salt stress treatment for 3 h, the two proteins interacted with each other and their localization remained unchanged.

3.4. The salt tolerance of alfalfa with overexpression of MsRCI2B or MsRCI2E genes

To assess the salt and alkali tolerance of individual RCI2 proteins and their interactions, MsRCI2B and MsRCI2E were separately transferred into yeast cells and co-transferred as MsRCI2B-RCI2E. Yeast growth was monitored on YPDA solid medium with varying NaCl concentrations (0, 100, 150, and 200 mmol/L) and pH levels (7, 7.5, 8, and 8.5) (Fig. S3). These results indicate that *MsRCI2B* and the *MsRCI2B-RCI2E* co-transfer groups exhibited greater salt and alkali tolerance than the *MsRCI2E* group.

To further investigate the effects of *MsRCI2E* and *MsRCI2B* on alfalfa growth and salt tolerance, we generated transgenic alfalfa lines over-expressing *MsRCI2E*, *MsRCI2B*, and *MsRCI2Em* (OE#*RCI2E*, OE#*RCI2B*, and OE#*RCI2Em*) (Fig. S4A). Additionally, we obtained transgenic alfalfa co-transformed with both *MsRCI2B* and *RCI2E* genes (OE#*RCI2B-2E*) to assess the synergistic effects on salt tolerance. Following selection with glyphosate, PCR verification (using the *bar* gene), and qPCR (using the *MsRCI2* genes), we isolated 5–7 independent transgenic lines (Fig. S4BC). Root fluorescence assays were conducted on *RCI2*-over-expressing lines with the fusion of fluorescent protein genes (*RCI2B*-

Cherry, *RCI2E-GFP*) (Fig. S4D). Transgenic alfalfa co-expressing *RCI2E* and *RCI2B* (OE#*RCI2B-2E1#*, 2#, and 12#) exhibited significantly higher expression levels of both genes than non-transgenic controls. Colocalization of Cherry and GFP fluorescence signals in the roots indicated successful coexpression.

For growth and salt tolerance analyses, we subjected *RCI2*-overexpressing alfalfa lines, including those coexpressing *RCI2B* and *RCI2E*, and non-transgenic control alfalfa (WT) to salt stress. Under control conditions, notable differences were observed in plant height, electrical conductivity, chlorophyll content, and branching number between some transgenic lines and WT ($p < 0.05$ or $p < 0.001$), particularly in the OE#*RCI2E* line (Fig. 3, Fig. S5). After 10 days of treatment with 200 mmol/L NaCl, WT growth was severely inhibited, exhibiting leaf wilting and near death. In contrast, transgenic alfalfa maintained better growth with fewer yellowed leaves (Fig. 3A). Differences in salt tolerance among transgenic lines were evident: OE#*RCI2E* had significantly higher plant height ($p < 0.001$), OE#*RCI2E* and OE#*RCI2B-2E* also exhibited higher chlorophyll content. Although the most salt-tolerant transgenic line remains uncertain, these results confirm that *RCI2B*, *RCI2E*, and the C-terminal deletion of *RCI2E*(*RCI2Em*) play distinct roles in alfalfa salt tolerance.

3.5. Homeostasis of reactive oxygen species was differently affected by the *MsRCI2s* gene under salt stress

The activities of antioxidant enzymes, including superoxide dismutase (SOD), catalase (CAT), and peroxidase (POD), as well as the proline, soluble sugar, and malondialdehyde (MDA) concentrations, were measured in all transgenic alfalfa lines (OE#) and wildtype lines (WT) under salt treatment (Fig. 3 and Fig. S5). Following salt treatment, both proline and soluble sugars increased significantly in all lines, with transgenic lines exhibiting markedly higher levels than the WT lines ($p < 0.001$) (Fig. S5DE). In contrast, SOD and POD activities were significantly higher in transgenic lines under untreated conditions. After salt treatment, SOD, POD, and CAT activities increased significantly in all transgenic lines and were markedly higher than those in the WT plants (Fig. 3C). However, the MDA levels were lower in the transgenic lines than in the WT lines (Fig. 3D).

In additional, the levels of H₂O₂ and oxygen free radicals (OFR) were measured, and diaminobenzidine (DAB), nitroblue tetrazolium (NBT) staining was performed (Fig. 3D, Fig. S5FG). Under untreated conditions, OE#*RCI2B* and OE#*RCI2B-2E* lines exhibited lower H₂O₂ levels than WT, while the OE#*RCI2E* line had higher OFR levels. After salt treatment, the H₂O₂ and OFR levels were significantly lower in all transgenic lines than in the WT, with DAB, and NBT staining, corroborating the changes observed in the H₂O₂ and OFR levels.

Although all transgenic lines demonstrated enhanced antioxidant capacity, variations were observed between them. Specifically, the OE#*RCI2E* line exhibited higher conductivity, H₂O₂ and OFR levels, and lower CAT enzyme activity than the OE#*RCI2B* and OE#*RCI2Em* lines. Thus, the presence of the C-terminal tail of *MsRCI2E* appears to reduce the gene's ROS-scavenging capacity, while interactions between RCI2B and RCI2E proteins may complement the function of the *RCI2E* gene.

3.6. Changes in ion homeostasis for various transgenic alfalfa under salt stress

To elucidate the mechanisms underlying salt tolerance in transgenic alfalfa, we comprehensively analyzed Na⁺, K⁺, and Na⁺/K⁺ ratios in the roots and leaves of both the transgenic and WT lines (Fig. 4AB). Under control conditions, K⁺ content varied significantly, with the OE#*RCI2Em* line exhibiting markedly lower K⁺ levels than WT ($p < 0.001$). A consistent pattern emerged after exposure to salt stress for 10 days: K⁺ content declined, Na⁺ content increased, and Na⁺/K⁺ ratios increased. All transgenic lines, except OE#*RCI2E*, notably exhibited significantly lower Na⁺ content and Na⁺/K⁺ ratios than the WT. Most lines did not exhibit

significant differences in root except OE#RCI2E-2B, which consistently displayed higher K⁺ content than other lines ($p < 0.01$). Furthermore, OE#RCI2B lines exhibited significantly elevated Na⁺/K⁺ ratios after stress ($p < 0.001$), indicating a unique response to salt stress in the root.

To gain insights into the molecular mechanisms underlying these changes in ion homeostasis, we analyzed the expression levels of the key ion transporter genes *MsSOS1*, *MsAKT1*, and *MsNHX1* (Fig. 4CD). *MsSOS1*, a plasma membrane Na⁺/H⁺ antiporter, consistently upregulated upon salt treatment, with OE#RCI2B and OE#RCI2Em lines exhibiting significantly higher *MsSOS1* expression than WT and other transgenic lines ($p < 0.001$). *MsAKT1*, a K⁺ transport channel, responds variably to salt stress in leaves and roots. In leaves, OE#RCI2B and OE#RCI2B-2E lines displayed the highest *MsAKT1* expression, which correlated with lower Na⁺/K⁺ ratios, suggesting efficient K⁺ uptake and transport. In roots, however, *MsAKT1* expression was highest in OE#RCI2B and OE#RCI2Em, with OE#RCI2B-2E showing the lowest. *MsNHX1*, a vacuole Na⁺/H⁺ antiporter, was most pronouncedly upregulated in OE#RCI2Em lines ($p < 0.001$). Overexpression of RCI2 genes

influences plasma membrane ion transporters and affects ion homeostasis under salt stress. Notably, *MsRCI2E* overexpression partially balanced ion homeostasis, albeit less effectively than *MsRCI2B*. The truncated RCI2Em variant demonstrated superior regulation, whereas the interaction between RCI2B and RCI2E appeared to compensate for the functional deficiencies in RCI2E.

We also assessed the expression of *MsRCI2A-2F* in each transgenic alfalfa line (Fig.S6). Overexpression of *MsRCI2B* or *MsRCI2Em* genes upregulates *MsRCI2A*, *MsRCI2D*, and *MsRCI2F* genes, whereas OE#RCI2E lines exhibited a significant decrease in *MsRCI2B* expression. After salt stress treatment, *MsRCI2A*, *MsRCI2D*, and *MsRCI2F* gene expression increased in OE#RCI2B and OE#RCI2Em lines. These findings suggest complex regulatory interactions among RCI2 genes, each fulfilling a distinct function without redundancy.

3.7. The function of *MsRCI2* protein interaction in salt tolerance

Regarding the interaction of the RCI2 protein, Kim et al. [27]

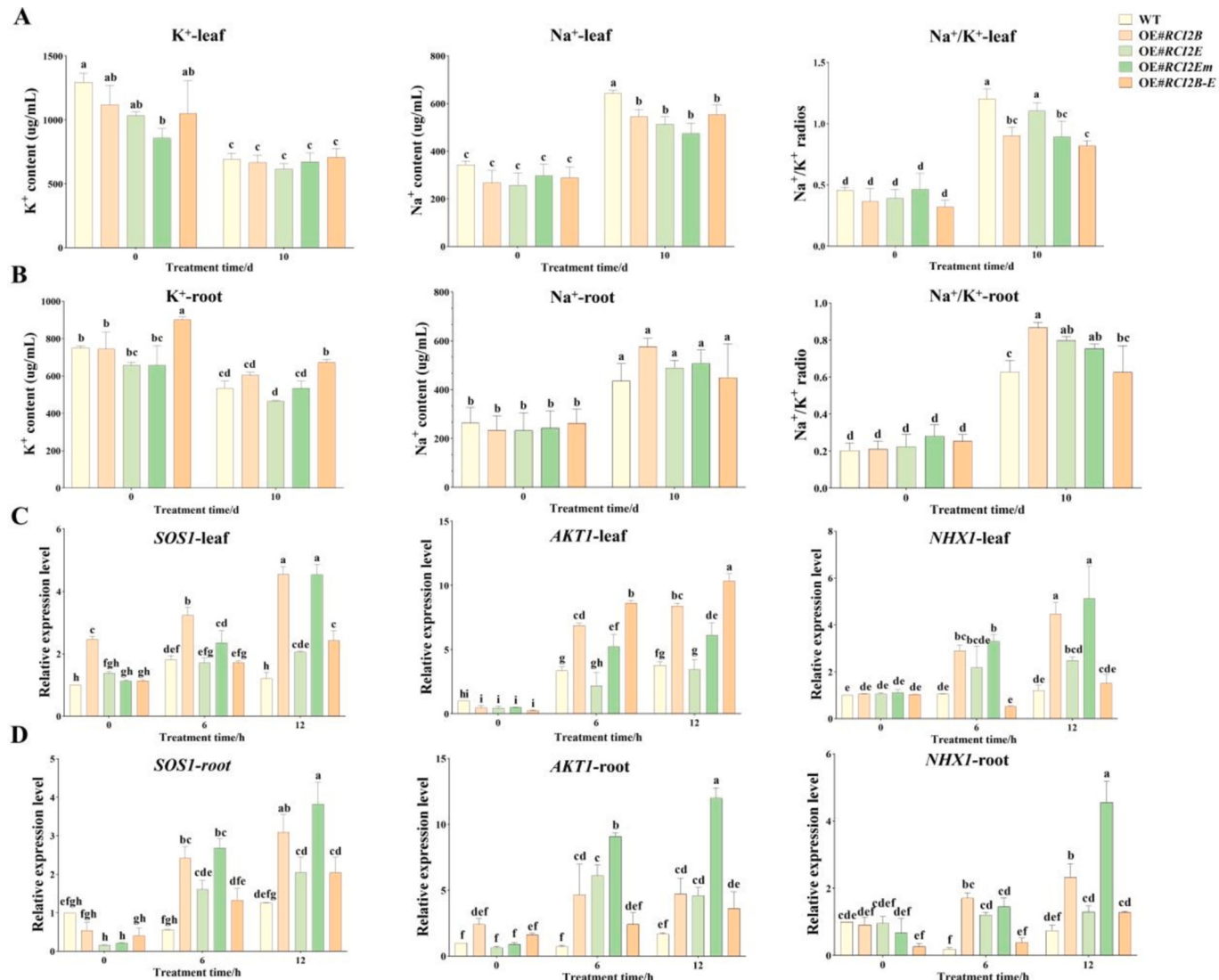


Fig. 4. Changes in sodium and potassium content and differential expression of ion transport related genes in transgenic plants under salt stress. (A-B) K⁺ and Na⁺ content, and Na⁺/K⁺ ratios in the leaves and roots of transgenic plants. (C-D) Expression levels of *SOS1*, *AKT1*, and *NHX1* genes in the leaves and roots of transgenic plants as measured by RT-qPCR. Each experiment was conducted in triplicate, with at least three technical replicates. Different letter indicates significant differences according to Duncan's multiple range test at $p < 0.05$ using One-way ANOVA.

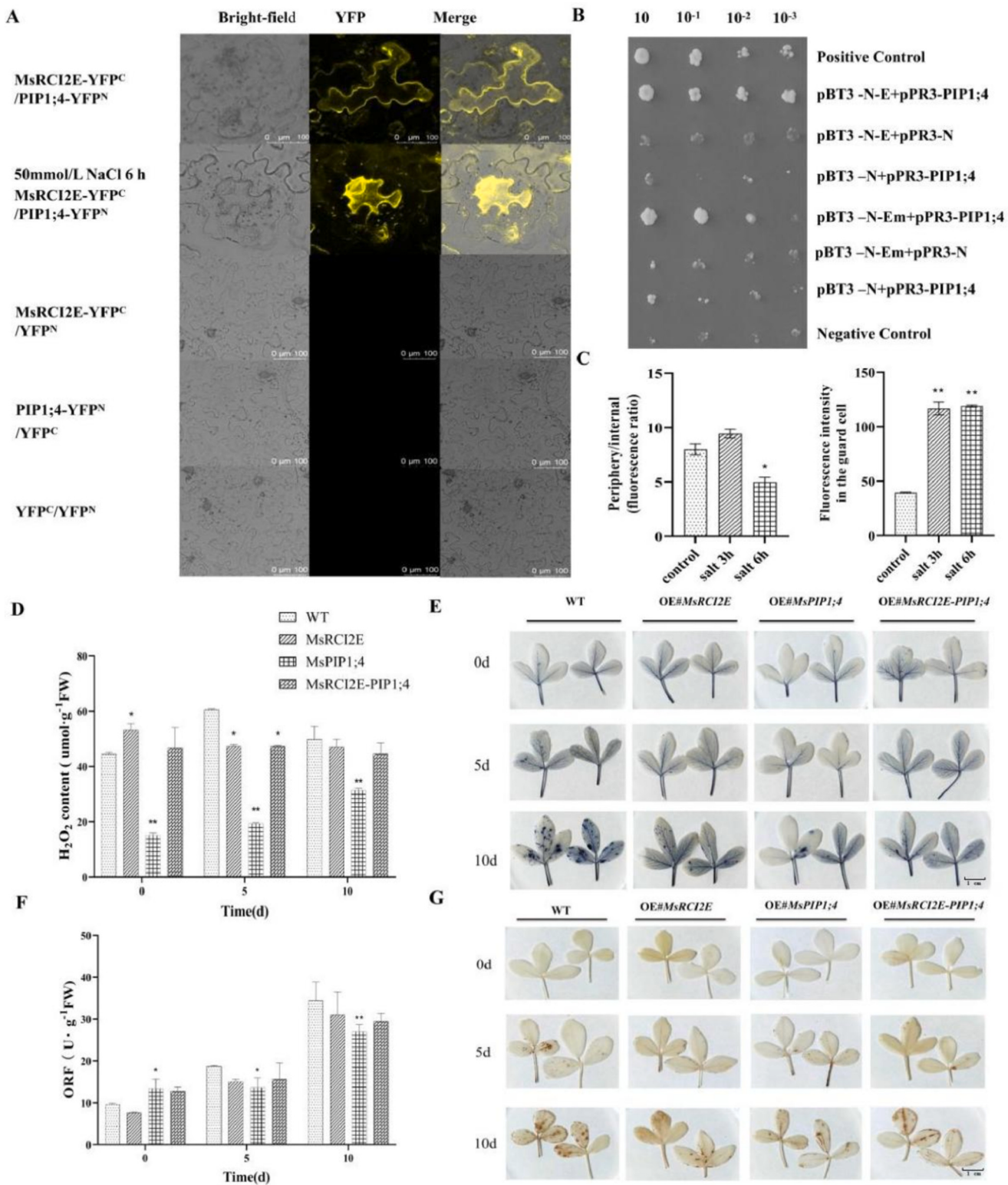


Fig. 5. Interaction of MsRCI2B/E with MsPIP1;4 and the function of protein interaction in salt tolerance.

(A) BiFC assay demonstrating the interaction between MsRCI2E and PIP1;4. The plasmid was co-expressed in tobacco leaves for 16 h, and fluorescence signals were observed before and after treatment with 50 mmol/L NaCl for 6 h.

(B) Yeast two-hybrid assays showing the interaction of PIP1;4 with MsRCI2E/Em.

(C) Comparison of fluorescence signal intensity inside and outside the membrane.

(D, E) H₂O₂ content and NBT staining of WT and transgenic lines (OE#) under salt stress.

(F, G) ORF content and DAB staining of WT and transgenic lines (OE#) under salt stress. Each experiment was conducted in triplicate, with at least three technical replicates. Statistical comparisons were performed using Tukey's test: *, p < 0.05; **, p < 0.01; ***, p < 0.001.

reported an association between MsRCI2E and MsRCI2F with CsPIP2; 1. To further explore this association, we employed a yeast two-hybrid approach to screen for plasma membrane proteins (PMPs) that specifically interact with MsRCI2B or MsRCI2E. Our findings revealed that MsCaM1 interacts with MsRCI2B, whereas MsPIP1;4 and MsHVP1 interact with MsRCI2E. These interactions were subsequently validated using the BiFC assay (Figs. 5A, 6A, S7), indicating that the interacting proteins were not solely confined to the plasma membrane but were also present within the cytoplasm. Notably, the MsPIP1;4-MsRCI2E interaction produced a yellow fluorescent ring proximal to the plasma membrane, suggesting a vesicular structure accompanied by additional fluorescence within the cell. Another, yeast two-hybrid experiments revealed that the interaction between MsRCI2Em and MsHVP1 was lost (Fig. 6B), while its interaction with MsPIP1;4 were notably weakened (Fig. 5B).

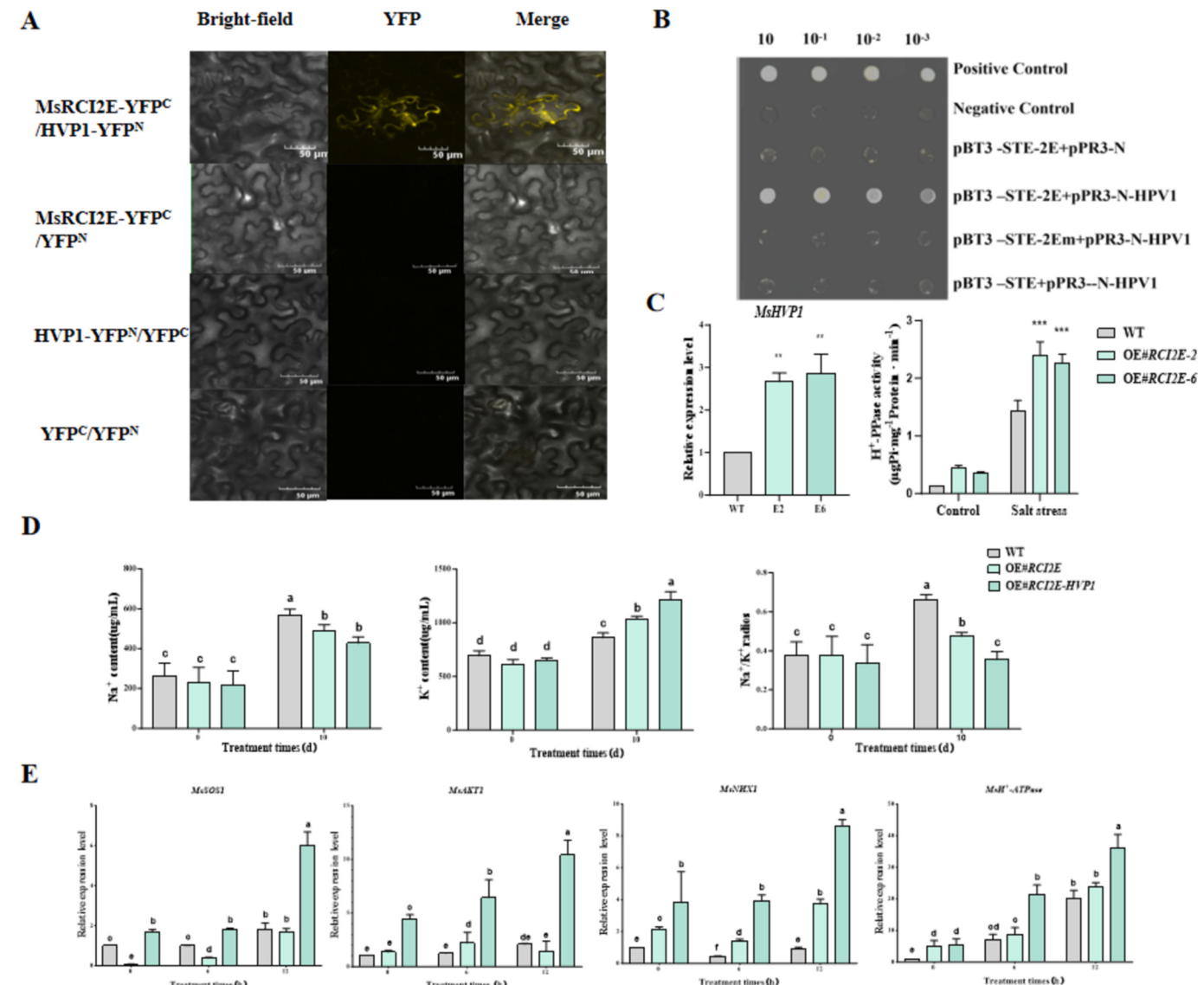


Fig. 6. Interaction of MsRCI2E with MsHVP1 and the role of protein interaction in salt tolerance.

(A) BiFC assay demonstrating the interaction between MsRCI2E and MsHVP1.

(B) Yeast two-hybrid assays showing the interaction of HVP1 with MsRCI2E/Em.

(C) Expression levels of *MsHVP1* gene and H⁺-PPase activity in WT and overexpression *MsRCI2E* transgenic alfalfa.

(D) Na⁺/K⁺ content and Na⁺/K⁺ ratios in the leaves of WT and transgenic plants (OE#) after salt stress.

(E) Expression levels of *MsSOS1*, *MsAKT1*, *MsNHX1*, and *MsH⁺-ATPase* genes in the leaves of WT and OE# after salt stress. Each experiment was conducted in triplicate, with at least three technical replicates. Different letter indicates significant differences according to Duncan's multiple range test at $p < 0.05$ using One-way ANOVA.

The results of DAB and NBT staining corroborated the measurements of H₂O₂ and OFR (Fig. 5EG). However, in the co-transformed lines (OE#RCI2E-PIP), there were no significant differences in H₂O₂ and OFR levels compared to the WT. Moreover, the activities of antioxidant enzymes SOD, POD, and CAT showed no significant differences between the OE#PIP1;4 and OE#RCI2E-PIP lines (Fig. S9B). The expression of the H₂O₂ production-related gene, *MsANN1*, did not differ significantly between the two lines (Fig. S9C). Given that neither H₂O₂ production nor ROS-scavenging enzyme activity differed significantly, the variation in H₂O₂ levels in the leaves may be related to its efflux. Based on the localization results of the interacting proteins MsPIP1;4 and MsRCI2E, it is inferred that the interaction between MsRCI2E and MsPIP1;4 is closely associated with the intracellular trafficking of PIP1;4 proteins. This interaction likely reduces PIP1;4 proteins on the plasma membrane and a diminished ability to export H₂O₂.

H⁺-PPases (proton-pumping pyrophosphatases, HVP) are a class of membrane-bound pyrophosphatases that generate energy by hydrolysing inorganic pyrophosphate (PPI) and transporting protons across the cell membrane [31]. More studies have indicated that H⁺-PPase plays a crucial role in plant resistance to abiotic stress [32]. In the OE#RCI2E transgenic lines, the expression of the *MsHVP1* gene was significantly upregulated, and the enzyme activity of H⁺-PPase was also significantly increased compared to WT plants (Fig. 6C). Thus, MsRCI2E positively regulated the function of H⁺-PPase under salt stress. Similarly, we obtained different transgenic lines and preliminarily determined the role of the interaction between MsRCI2E and HVP1 in the plant response to salt stress through differences in salt tolerance among transgenic lines. After salt stress treatment, the OE#RCI2E and OE#RCI2E-HVP lines exhibited higher levels of K⁺ compared to WT ($p < 0.01$, $p < 0.001$), along with elevated Na⁺ levels and Na⁺/K⁺ ratios (Fig. 6D). This indicated that the interaction between MsRCI2E and HVP1 enhanced the ion balance under salt stress and reduced Na⁺ influx. Additionally, the expression levels of ion channel-related genes such as *NHX1*, *PM-H⁺-ATPase*, *SOS1*, and *AKT1* were significantly higher in the OE#RCI2E-HVP line compared to the OE#RCI2E line and markedly higher than in WT (Fig. 6E). These findings suggest that the interaction between MsRCI2E and HVP1 plays a synergistic role in enhancing salt tolerance in alfalfa.

In summary, the interactions of MsRCI2E with MsPIP1;4 or HVP1 exerted distinct effects on the salt tolerance of alfalfa, highlighting the role of RCI2s in salt stress responses through interactions with membrane proteins.

4. Discussion

4.1. The special function of the C-terminal tail of the MsRCI2E protein

In alfalfa, there are six RCI2 genes that can be classified into tailless-type RCI2 (MsRCI2A-D, 54 amino acids) and tailed-type RCI2 (MsRCI2E, 76 amino acids) (Fig. S1). In *Arabidopsis*, tailless AtRCI2 (A-C) and AtRCI2H are found in the plasma membrane (PM), whereas tailed AtRCI2D is predominantly located in the endoplasmic reticulum (ER) [21]. Similarly, in *Camelina sativa*, tailless CsRCI2A is localised in the PM, whereas tailed CsRCI2D is found in both the membrane and cytosol, including the ER and endomembrane vesicles [19,33]. In alfalfa, tailless MsRCI2D [24] and MsRCI2B are localised to the PM, whereas tailed MsRCI2E is present in both the membrane and the cytosol (Fig. 1).

Renard et al. demonstrated that deletion of the C-terminal tail of SNA2 (mSNA2) shifts its localization from the PM to the ER, suggesting that the C-terminal tail may serve as a destination sequence that directs the protein to its correct location [34]. To investigate this, we truncated the C-terminus of MsRCI2E (MsRCI2Em). Analysis using mCherry fusion proteins revealed that MsRCI2Em, similar to the tailless MsRCI2B, was exclusively localised to the PM (Fig. 1). This finding indicated that the C-terminal tail significantly influenced the intracellular localization of RCI2 proteins.

In *Camelina*, CsRCI2D proteins lacking the tail complemented $\Delta pmp3$ yeast, but adding a C-terminal tail of CsRCI2D to a tailless RCI2 protein hindered its ability to complement NaCl tolerance in $\Delta pmp3$ yeast [19]. However, the functions of the C-terminal tail-deleted RCI2-overexpressing plants have not been extensively studied. We cloned *MsRCI2E* and its C-terminal tail-deletion variant, *MsRCI2Em*, and generated transgenic alfalfa lines overexpressing the *MsRCI2E* gene and *MsRCI2Em*. Salt tolerance evaluation revealed that OE#RCI2Em lines exhibited greater salt tolerance than OE#RCI2E lines, characterised by enhanced ROS scavenging and antioxidant capacity (Fig. 3) and improved ion homeostasis (Fig. 4).

The differing salt tolerance functions of *MsRCI2E* and *MsRCI2Em* may result from changes in cellular localization and variations in protein interactions or regulation. Our results revealed that MsRCI2E interacts with MsRCI2B, MsHVP1, and MsPIP1;4. Notably, deletion of the C-terminal tail in MsRCI2E results in the loss of interactions with MsRCI2B and MsHVP1, as well as a weakened interaction with MsPIP1;4, suggesting that the C-terminal tail is crucial for interactions with specific plasma membrane proteins. Additionally, differences in the expression of genes such as *MSSOS1*, *MsnHX1*, and *MsAKT1* between OE#MsRCI2E and OE#MsRCI2Em lines (Fig. 4) further emphasise the importance of the C-terminal tail in mediating *MsRCI2E*'s response to salt stress through its regulation of or interaction with membrane proteins.

4.2. Functional differences of MsRCI2B and MsRCI2E genes undergoing salt stress

RCI2 is crucial for various abiotic stress responses, particularly for regulating plant tolerance to cold, drought, alkaline, and salt stress [21]. However, within the same species, different RCI2 genes exhibit functional specificity [23]. In this study, both *MsRCI2B* and *MsRCI2E* responded to salt stress; however, their expression levels and trends differed significantly. Specifically, *MsRCI2B* exhibited higher expression levels than *MsRCI2E* under salt and alkaline stress (Fig. 1A). Additionally, overexpressing the *MsRCI2B* gene resulted in stronger salt tolerance compared to overexpressing *MsRCI2E*, as evidenced by higher soluble sugar accumulation, increased SOD and CAT activities, and lower ROS and MDA levels (Fig. 3). Furthermore, *MsRCI2B* better regulates ion homeostasis under salt stress, as indicated by its lower Na⁺/K⁺ ratio (Fig. 4). These differences may be attributed to disparities in gene structure, expression, regulation, and protein function [35].

The regulatory mechanisms of RCI2 expression remain underexplored, and no known transcription factors have been identified for these genes. Previous studies have indicated that overexpression of *MsRCI2* genes can regulate the expression of other *MsRCI2* genes [24,25]. This suggests a distinct regulatory mechanism between MsRCI2B and MsRCI2E. A yeast two-hybrid assay revealed that MsRCI2E interacts with MsRCI2B and MsRCI2D (Fig. S2). Still, none of the RCI2 proteins formed homodimers, indicating that regulatory relationships may be transcriptional or dependent on protein expression balance.

Several transgenic lines evidence indicate that functional specialisation among RCI2 paralogs is determined by differences in the activities of their cognate proteins. Liu et al. found reduced H⁺-ATPase activity and gene expression in *rci2a* mutants compared with wild-type and 35S: *MpRCI-rci2a* transgenic plants [12]. Our findings similarly showed that overexpressing *MsRCI2B* and *MsRCI2E* affected the expression of *MSSOS1*, *MsnHX1*, and *MsAKT1* genes, with OE#RCI2B lines showing significant upregulation compared to OE#RCI2E lines (Fig. 4). This suggests that the different regulatory patterns of *MsRCI2B* and *MsRCI2E* concerning ion transport genes contribute to their distinct functions in salt tolerance.

Two main factors contribute to the functional differences in salt tolerance between MsRCI2B and MsRCI2E. First, the C-terminal tail of MsRCI2E influenced its localization and protein interactions. As previously mentioned, deletion of this tail in *MsRCI2E* significantly enhanced

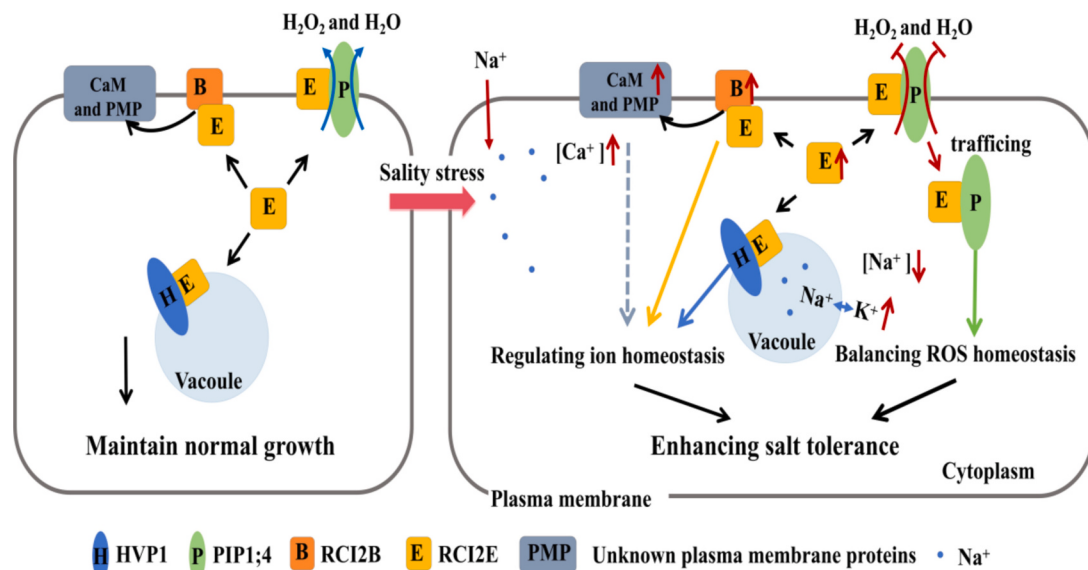


Fig. 7. Model of *MsRCI2B/E* genes response to salt stress. This model illustrates the interactions of *MsRCI2E* with *MsRCI2B*, *MsPIP1;4*, and *MsHVP1* to enhance salt tolerance by regulating ROS and ion homeostasis.

salt tolerance and improved antioxidant and ion homeostasis. Second, the specificity of interacting proteins is crucial. *MsRCI2B* interacts with CAM1, whereas *MsRCI2E* interacts with PIP1;4 and HVP1. These proteins are all involved in regulating ion transport and salt stress signalling [36–38]. The specificity of the protein interactions ultimately determines the functional diversity of RCI2 proteins.

4.3. The molecular mechanism by which *MsRCI2B* and *MsRCI2E* cooperatively regulate salt tolerance in alfalfa

Most researchers believe that, because of their small size, RCI2 cannot function as ion transporters on their own [39]. However, this does not preclude the possibility that the two RCI2 oligomers form transporters or interact with other membrane proteins. In this study, we found that *MsRCI2B* interacts with *MsRCI2E* but does not interact with itself. Upon interaction, these two proteins localised to the plasma membrane (Fig. 2). However, based on available data, it is difficult to determine whether their interaction leads to dimer formation or the establishment of an ion channel. Indeed, the ionic regulation capability of alfalfa co-transformed with *MsRCI2B* and *MsRCI2E* was not superior to that of the OE#*MsRCI2B* lines.

We compared the salt tolerance of various transgenic alfalfa lines, including those individually transformed with *MsRCI2B* or *MsRCI2E* and those co-transformed with both genes. The OE#*RCI2B-2E* lines exhibited higher levels of proline and soluble sugars and lower ROS compared to the OE#*RCI2E* lines (Fig. S5), and they showed the lowest Na⁺/K⁺ ratios (Fig. 4A). Additionally, the expression levels of *MsAKT1* in the leaves of OE#*MsRCI2B-2E* lines were significantly higher (Fig. 4CD). These observations suggest that the interaction between *MsRCI2B* and *MsRCI2E* may alleviate the negative regulatory effects of the C-terminal tail on plant salt tolerance and enhance alfalfa salt tolerance by modulating the expression of ion homeostasis-related genes.

RCI2 proteins play an important role in maintaining the ion balance, primarily through interactions with other proteins. Using *MsRCI2B* and *MsRCI2E* as bait in a yeast two-hybrid assay, we identified MsCaM1, which interacts with *MsRCI2B*; MsHVP1, which interacts with *MsRCI2E*; and MsPIP1;4, which interacts only with *MsRCI2E*. MsCaM1 is analogous to Arabidopsis CaM7 (At3g43810) [40]. Calmodulin (CaM) is ubiquitous in eukaryotes and is a highly conserved Ca²⁺ binding protein that plays multiple regulatory roles in response to various stimuli, including salt, cold, and drought stresses [41,42]. Therefore, the role of

the *MsRCI2B* in regulating ion homeostasis is closely linked to MsCaM1.

H⁺-PPases (proton-pumping pyrophosphatases, HVP) are a class of membrane-bound pyrophosphatases. In *Arabidopsis*, overexpression of *AVP1* leads to increased salt tolerance, primarily due to enhanced vacuole uptake of Na⁺, which mitigates the toxic effects of Na⁺ [43]. Our study found that the C-terminal tail of *MsRCI2E* is essential for its interaction with *MsHVP1*. Co-transformation of *RCI2E* and *HVP1* enhanced ion homeostasis regulation and reflected lower Na⁺/K⁺ ratios. This co-transformation also positively regulated the expression of key genes, such as *MsSOS1*, *MsHKT1*, *MsNHX1*, and *MsH⁺-ATPase* (Fig. 6), suggesting that *MsRCI2E* collaboratively regulates ion homeostasis through its interaction with *MsHVP1*.

Interestingly, *MsRCI2E*'s interaction with *MsPIP1;4* was localised near the plasma membrane, within vesicles, and in the cytoplasm, after salt treatment, interaction proteins trafficking into cytoplasm. While the C-terminal tail of *RCI2E* is not essential for this interaction, its absence weakens binding. Co-transformation with *MsPIP1;4* and *MsRCI2E* enhanced antioxidant enzyme activity; however, the H₂O₂ content in the leaves did not significantly differ from that in the wild-type (Fig. 5D). Research indicates that PIP2 facilitates water permeability. In contrast, PIP1's water transport capability remains controversial [44]. PIPs also exhibit broad-channel activity for various small molecules, including glycerol, CO₂, and H₂O₂ [45,46]. Zhang et al. found that OsPIP2 enhances H₂O₂ permeability under alkaline stress [47]. Furthermore, studies show that AtPIP2 transports H₂O₂ into the cytoplasm via endocytosis under hyperosmotic stress [48]. The diversity of the PIP protein function may explain the unique findings of the present study. In this study, we revealed that under normal conditions, *MsPIP1;4* is predominantly localised in vesicle-like structures near the plasma membrane. However, following salt stress treatment, *MsPIP1;4* was re-localised to the cytoplasm and guard cells of the stomata (Fig. S8). This dynamic shift in localization closely resembles the behavior of *Arabidopsis* PIP2; 1, as previously reported [49]. In addition, *MsPIP1;4* facilitates H₂O₂ efflux, and before and after salt stress treatment, the OE#*PIP1;4* lines showed lower H₂O₂ levels in leaves. The interaction between *MsRCI2E* and *MsPIP1;4* assists the intracellular trafficking of *MsPIP1;4*, leading to reduced *PIP1;4* protein levels in the plasma membrane and diminished H₂O₂ efflux. Despite the higher antioxidant enzyme activity, intracellular H₂O₂ accumulation remains notable. H₂O₂ acts as both a reactive oxygen species and a signalling molecule. Thus, the *MsRCI2E*-*MsPIP1;4* interaction under salt stress may not be negative. Since

MsRCI2B also interacts with MsRCI2E, we speculate that interactions among these three proteins may maintain a balance, ensuring PIP1;4 homeostasis at the plasma membrane and regulating intracellular H₂O₂ levels.

In summary, MsRCI2B is localised to the plasma membrane, where it interacts with proteins such as calmodulin (CaM) and MsRCI2E. In contrast, MsRCI2E is present in both the plasma membrane and cytoplasm, interacting with the aquaporin PIP1;4 and the vacuolar proton pump HVP1. Under salt stress, increased Na⁺ influx raises cytosolic Ca²⁺ levels, activating CaM to regulate ion homeostasis. Meanwhile, MsRCI2E enhances HVP1 activity, promoting Na⁺ sequestration into vacuoles and reducing cytoplasmic ion toxicity. Additionally, MsRCI2E assists PIP1;4 trafficking from plasma membrane to cytoplasm, limiting H₂O₂ and water efflux, which helps maintain ROS balance and prevent water loss. The interaction between MsRCI2B and MsRCI2E may further modulate MsRCI2E's function, enhancing plant salt stress tolerance (Fig. 7).

CRediT authorship contribution statement

Depeng Zhang: Writing – review & editing, Writing – original draft, Methodology, Investigation, Formal analysis. **Zhongbao Shen:** Resources, Project administration, Funding acquisition, Conceptualization. **Pin He:** Visualization, Methodology, Investigation, Formal analysis. **Jianli Wang:** Methodology, Investigation, Formal analysis. **Donghuan Li:** Visualization, Methodology, Investigation, Formal analysis. **Jing Meng:** Investigation, Formal analysis. **Dongmei Zhang:** Investigation, Formal analysis. **Jia You:** Visualization, Formal analysis. **Yaqin Luo:** Visualization, Formal analysis. **Xinsheng Wang:** Methodology, Formal analysis. **Xu Zhuang:** Investigation. **Linlin Mu:** Investigation. **Shichao Zhang:** Formal analysis. **Weibo Han:** Project administration, Funding acquisition, Conceptualization. **Hua Cai:** Writing – review & editing, Supervision, Project administration, Funding acquisition, Conceptualization.

Declaration of competing interest

The authors declare that they have no known competing financial interests or personal relationships that could have appeared to influence the work reported in this paper.

Acknowledgements

This research was financially supported by the National Natural Science Foundation of China (32071866), and the Science and Technology Innovation 2030-Major Project (2022ZD040120401).

Appendix A. Supplementary data

Supplementary data to this article can be found online at <https://doi.org/10.1016/j.ijbiomac.2025.140093>.

References

- [1] Rahma Goussi, Arafet Manaa, Walid Derbali, Simone Cantamessa, Chedly Abdelly, Roberto Arbato, Comparative analysis of salt stress, duration and intensity, on the chloroplast ultrastructure and photosynthetic apparatus in *Thellungiella salsuginea*, *J. Photochem. Photobiol. A* 183 (2018) 275–287, <https://doi.org/10.1016/j.jphotobiol.2018.04.047>.
- [2] C.W. Bourque, Central mechanisms of osmosensation and systemic osmoregulation [J], *Nat. Rev. Neurosci.* 9 (7) (2008) 519–531.
- [3] C. Chen, W. Yu, X. Xu, Y. Wang, B. Wang, S. Xu, Q. Lan, Y. Wang, Research advancements in salt tolerance of Cucurbitaceae: from salt response to molecular mechanisms, *Int. J. Mol. Sci.* 25 (16) (2024) 9051, <https://doi.org/10.3390/ijms25169051>.
- [4] J.K. Zhu, Salt and drought stress signal transduction in plants, *Annu. Rev. Plant Biol.* 53 (2008) 247–273, <https://doi.org/10.1146/annurev.aplant.53.091401.143329>.
- [5] J.K. Zhu, Abiotic stress signaling and responses in plants, *Cell* 167 (2) (2016) 313–324, <https://doi.org/10.1016/j.cell.2016.08.029>.
- [6] Aimin Lv, Liantai Su et al. The MsDHN1-MsPIP2; 1-Msm MYB module orchestrates the trade-off between growth and survival of alfalfa in response to drought stress.
- [7] M. Cui, Y. Li, J. Li, et al., Ca²⁺-dependent TaCCD1 cooperates with TaSAUR215 to enhance plasma membrane H⁺-ATPase activity and alkali stress tolerance by inhibiting PP2C-mediated dephosphorylation of TaHA2inwheat[J], *Mol. Plant* 16 (3) (2023) 571–587, <https://doi.org/10.1016/j.molp.2023.01.010>.
- [8] Xia Lingfeng, M. Mar, et al., Unusual roles of secretory SNARE SYP132 in plasma membrane H⁺-ATPase traffic and vegetative plant growth.[J], *Plant Physiol.* (2019), <https://doi.org/10.1104/pp.19.00266>.
- [9] Shuhan Yu, Jiaxuan Wu, Yanmei Sun, Haifeng Zhu, Qiguo Sun, Pengcheng Zhao, Risheng Huang, and Zhenfei Guo Acalmodulin-like protein (CML10) interacts with cytosolic enzymes GSTU8 and FBA6 to regulate coldtolerance.
- [10] S. Mitsuya, M. Taniguchi, H. Miyake, T. Takabe, Overexpression of *RCI2A* decreases Na⁺ uptake and mitigates salinity-induced damages in *Arabidopsis thaliana* plants, *Physiol. Plant.* 128 (2006) 95–102, <https://doi.org/10.1111/j.1399-3054.2006.00714.x>.
- [11] S. Mitsuya, M. Taniguchi, H. Miyake, T. Takabe, Disruption of *RCI2A* leads to over-accumulation of Na⁺ and increased salt sensitivity in *Arabidopsis thaliana* plants, *Planta* 222 (2005) 1001–1009, <https://doi.org/10.1007/s00425-005-0043-9>.
- [12] B. Liu, D. Feng, B. Zhang, P. Mu, Y. Zhang, Y. He, et al., Musaparadisica RCI complements AtRCI and confers Na⁺ tolerance and K⁺ sensitivity in *Arabidopsis*, *Plant Sci.* 184 (2012) 102–111, <https://doi.org/10.1016/j.plantsci.2011.12.004>.
- [13] S.H. Kim, J.Y. Kim, S.J. Kim, K.S. An, G. An, S.R. Kim, Isolation of cold stress-responsive genes in the reproductive organs, and characterization of the OsLti6b gene from rice (*Oryza sativa L.*), *Plant Cell Rep.* 26 (2007) 1097–1110, <https://doi.org/10.1007/s00299-006-0297-0>.
- [14] V. Sivankalyani, M. Geetha, K. Subramanyam, S. Girija, Ectopic expression of *Arabidopsis RCI2A* gene contributes to cold tolerance in tomato, *Transgenic Res.* 24 (2015) 237–251, <https://doi.org/10.1007/s11248-014-9840-x>.
- [15] P.S. Rocha, Plant abiotic stress-related RCI2/PMP3s: multigenes for multiple roles, *Planta* 243 (2016) 1–12, <https://doi.org/10.1007/s00425-015-2386-1>.
- [16] R.K. Yeshvekar, R.B. Nitinavare, T. Chakradhar, P. Bhatnagar-Mathur, M.K. Reddy, P.S. Reddy, Molecular characterization and expression analysis of pearl millet plasma membrane proteolipid 3 (ppm 3) genes in response to abiotic stress conditions, *Plant Gene* 10 (2017) 37–44, [https://doi.org/10.1016/j.pgen.2017.05.002 DOI](https://doi.org/10.1016/j.pgen.2017.05.002).
- [17] Y. Zhou, L. Ge, G. Li, P. He, Y. Yang, S. Liu, In silico identification and expression analysis of Rare Cold Inducible 2 (RCI2) gene family in cucumber, *J. Plant Biochem. Biotechnol.* 29 (2020) 56–66, [https://doi.org/10.1007/s13562-019-00510-6 DOI](https://doi.org/10.1007/s13562-019-00510-6).
- [18] L. Li, N. Li, S.F. Song, Y.X. Li, X.J. Xia, X.Q. Fu, G.H. Chen, H.F. Deng, Cloning and characterization of the drought-resistance OsRCI2-5 gene in rice (*Oryza sativa L.*), *Genetics Mol Res* 13 (2014) 4022–4035, <https://doi.org/10.4238/2014.May.23.13>.
- [19] H. Kim, J. Lee, H. Jang, et al., *CsRCI2A* and *CsRCI2E* genes show opposite salt sensitivity reaction due to membrane potential control [J], *Acta Physiol. Plant.* 38 (2) (2016).
- [20] J. Fu, D.F. Zhang, Y.H. Liu, S. Ying, Y.S. Shi, Y.C. Song, et al., Isolation and characterization of maize PMP3 genes involved in salt stress tolerance, *PloS One* 7 (2012) e31101, <https://doi.org/10.1371/journal.pone.0031101>.
- [21] J. Medina, M.L. Ballesteros, J. Salinas, Phylogenetic and functional analysis of *Arabidopsis RCI2* genes, *J. Exp. Bot.* 58 (2007) 4333–4346, <https://doi.org/10.1093/jxb/erm285>.
- [22] R. Long, F. Zhang, Z. Li, M. Li, L. Cong, J. Kang, et al., Isolation and Functional Characterization of Salt-Stress Induced RCI2-like Genes from *Medicago Sativa* and *Medicago*, 2015.
- [23] S.C. Brunetti, M.K.M. Arseneault, P.J. Gulick, Characterization of the Esi 3/RCI2/PMP3 gene family in the Triticeae [J], *BMC Genomics* 19 (2018) 898.
- [24] C. Li, T. Song, L. Zhan, C. Cong, H. Xu, L. Dong, H. Cai, Overexpression of MsRCI2A, MsRCI2B, and MsRCI2C in alfalfa (*Medicago sativa L.*) provides different extents of enhanced alkali and salt tolerance due to functional specialization of MsRCI2s, *Front. Plant Sci.* 12 (2021) 702195, <https://doi.org/10.3389/fpls.2021.702195>.
- [25] Zhang, D.; Zhang, Z.; Li, C.; Xing, Y.; Luo, Y.; Wang, X.; Li, D.; Ma, Z.; Cai, H. Overexpression of MsRCI2D and MsRCI2E enhances salt tolerance in Alfalfa (*Medicago sativa L.*) by stabilizing antioxidant activity and regulating ion.
- [26] C.A. Schneider, W.S. Rasband, K.W. Eliceiri, NIH Image to Image J: 25 years of image analysis [J], *Nat. Methods* 9 (7) (2012) 671–675.
- [27] H.-S. Kim, W. Park, H.-G. Lim, S. Eom, J.-H. Lee, J.E. Carlson, et al., NaCl-Induced CsRCI2E and CsRCI2F Interact with Aquaporin CsPIP2; 1 to Reduce Water Transport in *Camelina sativa L.*, 2019.
- [28] A. Rahman, Y. Kawamura, M. Maeshima, A. Rahman, M. Uemura, Plasma membrane aquaporin members PIPs act in concert to regulate cold acclimation and freezing tolerance responses in *Arabidopsis thaliana*, *Plant Cell Physiol.* 61 (4) (2020) 787–802, <https://doi.org/10.1093/pcp/pcaa005>.
- [29] B. Otto, N. Uehlein, S. Sdorra, M. Fischer, M. Ayaz, X. Belastegui-Macadam, M. Heckwolf, M. Lachnit, N. Pede, N. Priem, A. Reinhard, S. Siegfart, M. Urban, R. Kaldenhoff, Aquaporin tetramer composition modifies the function of tobacco aquaporins, *J. Biol. Chem.* 285 (41) (2010) 31253–31260, <https://doi.org/10.1074/jbc.M110.115881>.
- [30] A. Sommer, B. Geist, O. Da Ines, R. Gehwolf, A.R. Schäffner, G. Obermeyer, Ectopic expression of *Arabidopsis thaliana* plasma membrane intrinsic protein 2 aquaporins in lily pollen increases the plasma membrane water permeability of

- grain but not of tube protoplasts, *New Phytol.* 180 (4) (2008) 787–797, <https://doi.org/10.1111/j.1469-8137.2008.02607.x>.
- [31] J. Su, T. Bai, F. Wang, et al., Overexpression of *Arabidopsis H⁺-pyrophosphatase* improves the growth of alfalfa under long-term salinity, drought conditions and phosphate deficiency [J], *Czech J. Genet. Plant Breed.* 55 (4) (2019) 156–161.
- [32] X. Wang, H. Wang, S. Liu, et al., Genetic variation in ZmVPP1 contributes to drought tolerance in maize seedlings [J], *Nat. Genet.* 48 (10) (2016) 1233–1241.
- [33] H. Kim, J. Shin, H. Lee, et al., CsRCI2D enhances high-temperature stress tolerance in *Camellia sativa* L. through endo-membrane trafficking from the plasma membrane [J], *Plant Sci.* 320 (2022) 111294.
- [34] H.F. Renard, D. Demaegd, B. Guerriat, P. Morsomme, Efficient ER exit and vacuole targeting of yeast Sna 2p require two tyrosine-based sorting motifs, *Traffic* 11 (2010) 931–946, <https://doi.org/10.1111/j.1600-0854.2010.01070.x>.
- [35] H. Smith, Signal perception, differential expression within multigene families and the molecular basis of phenotypic plasticity [J], *Plant Cell Environ.* 13 (7) (2010) 585–594.
- [36] X. Li, X. Wang, Y. Yang, et al., Single-molecule analysis of PIP2;1 dynamics and partitioning reveals multiple modes of *Arabidopsis* plasma membrane aquaporin regulation [J], *Plant Cell* 23 (10) (2011) 3780–3797, <https://doi.org/10.1105/tpc.111.091454>.
- [37] Y. Zhang, X. Feng, L. Wang, et al., The structure, functional evolution, and evolutionary trajectories of the H⁺-PPase gene family in plants [J], *BMC Genomics* 21 (1) (2020).
- [38] Mingxue Chu, Jiaoqiao Li, Jingyu Zhang, Sufen Shen, Cuina Li, Yingjie Gao, Suqiao Zhang, AtCaM4 interacts with a Sec 14-like protein, PATL1, to regulate freezing tolerance in *Arabidopsis* in a CBF-independent manner, *J. Exp. Bot.* 69 (21) (2018) 5241–5253, <https://doi.org/10.1093/jxb/ery278>.
- [39] H.S. Kim, W. Park, H.S. Lee, J.H. Shin, S.J. Ahn, Subcellular journey of rare cold inducible 2 protein in plant under stressful condition, *Front. Plant Sci.* 11 (2021) 610251, <https://doi.org/10.3389/fpls.2020.610251>.
- [40] Q. Zeb, X. Wang, C. Hou, X. Zhang, M. Dong, S. Zhang, Q. Zhang, Z. Ren, W. Tian, H. Zhu, L. Li, L. Liu, The interaction of CaM7 and CNGC14 regulates root hair growth in *Arabidopsis*, *J Integr Plant Biol.* 62 (7) (2020) 887–896, doi:10.1111/jipb.12890.Epub.
- [41] R. Kushwaha, A. Singh, Chattopadhyay S. Calmodulin 7 plays an important role as transcriptional regulator in *Arabidopsis* seedling development, *Plant Cell.* 20 (7) (2008) 1747–1759, <https://doi.org/10.1105/tpc.107.057612.Epub>.
- [42] M. Chu, J. Li, J. Zhang, S. Shen, C. Li, Y. Gao, S. Zhang, AtCaM4 interacts with a sec 14-like protein, PATL1, to regulate freezing tolerance in *Arabidopsis* in a CBF-independent manner, *J. Exp. Bot.* 69 (21) (2018) 5241–5253, <https://doi.org/10.1093/jxb/ery278>.
- [43] R.K. Schilling, M. Tester, P. Marschner, et al., AVP1: one protein, many roles [J], *Trends Plant Sci.* 22 (2) (2017) 154–162.
- [44] V. Van Wilder, U. Miecielica, H. Degand, R. Derua, E. Waelkens, F. Chaumont, Maize plasma membrane aquaporins belonging to the PIP1 and PIP2 subgroups are in vivo phosphorylated, *Plant Cell Physiol.* 49 (9) (2008) 1364–1377, <https://doi.org/10.1093/pcp/pcn112>.
- [45] K. Varadaraj, S.S. Kumari, Lens aquaporins function as peroxiporins to facilitate membrane transport of hydrogen peroxide, *Biochem. Biophys. Res. Commun.* 524 (4) (2020) 1025–1029, <https://doi.org/10.1016/j.bbrc.2020.02.031>.
- [46] Q. Chen, R. Liu, Y. Wu, S. Wei, Q. Wang, Y. Zheng, R. Xia, X. Shang, F. Yu, X. Yang, L. Liu, X. Huang, Y. Wang, Q. Xie, ERAD-related E2 and E3 enzymes modulate the drought response by regulating the stability of PIP2 aquaporins, *Plant Cell* 33 (8) (2021) 2883–2898, <https://doi.org/10.1093/plcell/koab141>.
- [47] H. Zhang, F. Yu, P. Xie, S. Sun, X. Qiao, S. Tang, C. Chen, S. Yang, C. Mei, D. Yang, Y. Wu, R. Xia, X. Li, J. Lu, Y. Liu, X. Xie, D. Ma, X. Xu, Z. Liang, Z. Feng, X. Huang, H. Yu, G. Liu, Y. Wang, J. Li, Q. Zhang, C. Chen, Y. Ouyang, Q. Xie, A Gy protein regulates alkaline sensitivity in crops, *Science* 379 (2023) (6638): eade 8416. doi: 10.1126/science.adc8416. Epub 2023 Mar 24. PMID: 36952416.
- [48] M.M. Wudick, X. Li, V. Valentini, N. Geldner, J. Chory, J. Lin, C. Maurel, D.T. Luu, Subcellular redistribution of root Aquaporins induced by hydrogen peroxide, *Mol. Plant* 8 (7) (2015) 1103–1114, <https://doi.org/10.1016/j.molp.2015.02.017>.
- [49] X. Li, X. Wang, Y. Yang, R. Li, Q. He, X. Fang, D.T. Lu, C. Maurel, J. Lin, Single-molecule analysis of PIP2;1 dynamics and partitioning reveals multiple modes of *Arabidopsis* plasma membrane aquaporin regulation, *Plant Cell* 23 (2011) 3780–3797, <https://doi.org/10.1105/tpc.111.091454>.